Europhysics Letters PREPRINT

## Liquid-vapor phase separation in a thermocapillary force field

D. Beysens  $^1(^*)$ , Y. Garrabos  $^2$ , V. S. Nikolayev  $^1$ , C. Lecoutre-Chabot  $^2$ , J.-P. Delville  $^3$  and J. Hegseth  $^4$ 

CNRS, Université de Bordeaux I, Cours de la Libération, 33405 Talence Cedex, France

<sup>4</sup> Department of Physics, University of New Orleans, New Orleans, Louisiana 70148,
USA

PACS. 68.35.Rh - Phase transitions and critical phenomena.

PACS. 44.35.+c - Heat flow in multiphase systems.

PACS. 68.03.Cd - Surface tension and related phenomena.

Abstract. — We study the growth of gas bubbles surrounded by liquid during the phase separation of a pure  $\mathrm{CO}_2$  sample quenched from one-phase to two-phase region of the phase diagram by rapid cooling in microgravity. The vicinity of the critical point ensures slowing-down of the growth process. The bubble growth by coalescence is modified by local laser heating. It induces a thermocapillary (Marangoni) effect that attracts the bubbles towards the center of the beam. At the beginning of the phase separation, a bubble is trapped there and "captures" the surrounding bubbles. The growth exponent for the central bubble radius is close to 0.5, while that for the other bubbles is 1/3. We present a theoretical model that explains the experimental data and justifies that the temperature can vary along the gas-liquid interface in a pure fluid during its phase separation.

Introduction. — On earth, phase separation processes in liquids are strongly affected by gravity. The density difference between the evolving phases leads to sedimentation and formation of layered structure. Under microgravity, Marangoni convection resulting from induced temperature gradients at the surface of the emerging drops can become predominant. These temperature gradients result in interfacial tension gradients that are known to cause linear motion of droplets (thermocapillary migration) [1]. The resulting flow generally increases the rate of collisions between the drops and thus the rate of coalescences. Such a phenomenon has already been observed in microgravity during sounding rocket flights [2]. However, due to the short duration of the experiments, the expected thermocapillary-driven coarsening regime

<sup>&</sup>lt;sup>1</sup> ESEME, Service des Basses Températures, DSM/DRFMC, CEA-Grenoble, France(\*\*)

<sup>&</sup>lt;sup>2</sup> CNRS-ESEME, Institut de Chimie de la Matière Condensée de Bordeaux, 87, Avenue du Dr. Schweitzer, 33608 Pessac Cedex, France

<sup>&</sup>lt;sup>3</sup> Centre de Physique Moléculaire, Optique et Hertzienne,

<sup>(\*)</sup> E-mail: dbeysens@cea.fr

<sup>(\*\*)</sup> Mailing address: CEA-ESEME, Institut de Chimie de la Matière Condensée de Bordeaux, 87, Avenue du Dr. Schweitzer, 33608 Pessac Cedex, France

<sup>©</sup> EDP Sciences

2 EUROPHYSICS LETTERS

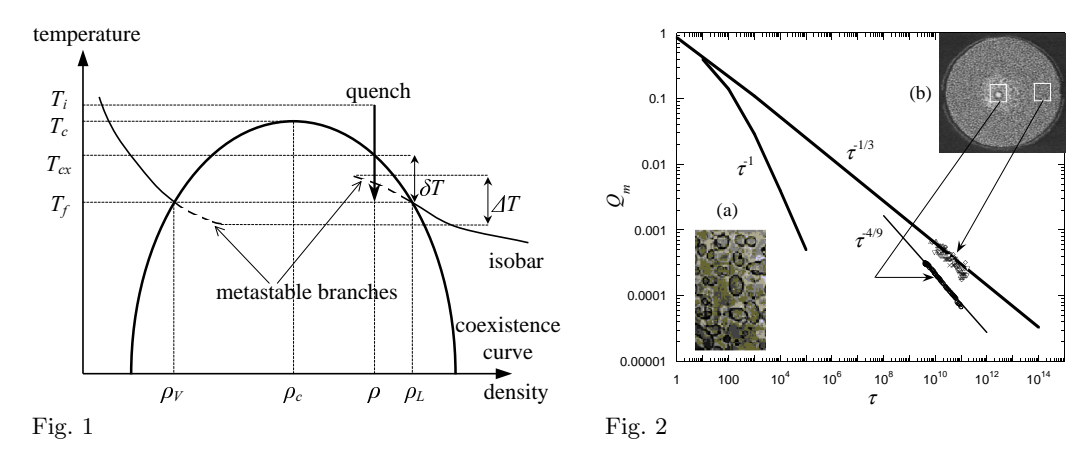


Fig. 1 – Schematic phase diagram for simple fluids in the coordinates temperature-density. The isobar that corresponds to the final fluid state  $T_f$  is shown with its metastable branches.

Fig. 2 – Growth laws of phase separating fluid close to the critical point in the reduced coordinates (inverse length  $Q_m$ , time  $\tau$ ). The experimental points illustrate the growth of the central single bubble for  $\delta T = 85, 90, 100$  mK with the exponent close to -0.5 while the  $Q_m(\tau) \sim \tau^{-1/3}$  behavior is recovered far from the illuminated area. The fit using the theoretical  $-4/9 \approx -0.44$  exponent is also shown.

lasts roughly 15 s, which is not long enough. By performing experiments on board the Mir space station, we are able to observe the droplet coarsening during 13 hours which corresponds to almost two decades in reduced time. To avoid coupling with the temperature changes associated with the quenching procedure, Marangoni flows are here created in the sample with a He-Ne laser passing through the small central part of the sample.

A phase separation experiment consists of quenching a pure fluid (here  $CO_2$ ) from the initial single-phase state  $(\rho, T_i)$  to another state  $(\rho, T_f)$  where homogeneous stability is lost and phase separation occurs ( $\rho$  is the mean density of the fluid sample cell,  $T_i$  is the initial temperature, and  $T_f$  is the final temperature). As illustrated in Fig. , the evolution of the system is defined by the relationship between the critical temperature  $T_c$ , the coexistence temperature  $T_{cx}$ , and the quench depth  $\delta T = T_{cx} - T_f$ . Depending on the final (equilibrium) volume fraction  $\phi$  of the minority phase, the phase transition may proceed either by the growth of isolated droplets when  $\phi < 30\%$  (insert (b) in Fig. 2) or by growth of interconnected domains when  $\phi > 30\%$  (insert (a) in Fig. 2).

The characteristic size of the evolving pattern  $L_m$  as a function of time t can be characterized [3] in terms of the reduced coordinates  $Q_m = 2\pi \xi^-/L_m$  and  $\tau = t/t_\xi$ , where  $\xi^-$  and  $t_\xi = 6\pi \eta_o(\xi^-)^3/k_B T_f$  are, respectively, the correlation length of the density fluctuations inside the coexistence curve and the associated relaxation time scale,  $\eta_o$  being the fluid viscosity. In off-critical systems (isolated domains, Fig. 2), a behavior  $Q_m(\tau) = 0.95 \tau^{-1/3}$  has been measured over more than seven decades in time [3] independently of the quench depth.

Experimental. – The CO<sub>2</sub> fluid (supplied by Air Liquide, with purity better than 99.998%) is enclosed between two transparent sapphire windows and a copper alloy cylindrical cell (11.6 mm internal diameter, thickness L=1.49 mm). The cell is set in a high precision thermostat (  $\pm 50~\mu \rm K$  accuracy) which is located inside the ALICE instrument [4] onboard the Mir station. The experimental cell is filled at the density  $\rho=1.094~\rho_c$ , where  $\rho_c$  is the critical density. Ini-

tially, the fluid temperature is above the critical temperature, and the fluid is homogeneous. The sample is then thermally quenched below the coexistence curve, the total quench duration being about 10 s. The cell is illuminated by white light parallel to the cylindrical cell walls. A CCD video camera captures images of the entire volume, the depth of field being larger than the sample thickness. A He-Ne laser beam (power P=1 mW, wavelength 632.8 nm in vacuum, beam diameter  $2\omega=300~\mu\text{m}$ ) propagates along the axis of the cell. Sapphire and CO<sub>2</sub> are transparent at this wavelength. However, a weak part  $\gamma\approx 2\cdot 10^{-6}$  [5] of the beam power is absorbed per window. As a consequence, the light beam induces a weak temperature gradient in the fluid.

Our phase separation experiments were carried out for the quench depths  $\delta T = 85$ , 90, and 100 mK. As illustrated in Fig. 3a, a single drop emerges and grows rapidly in the beam

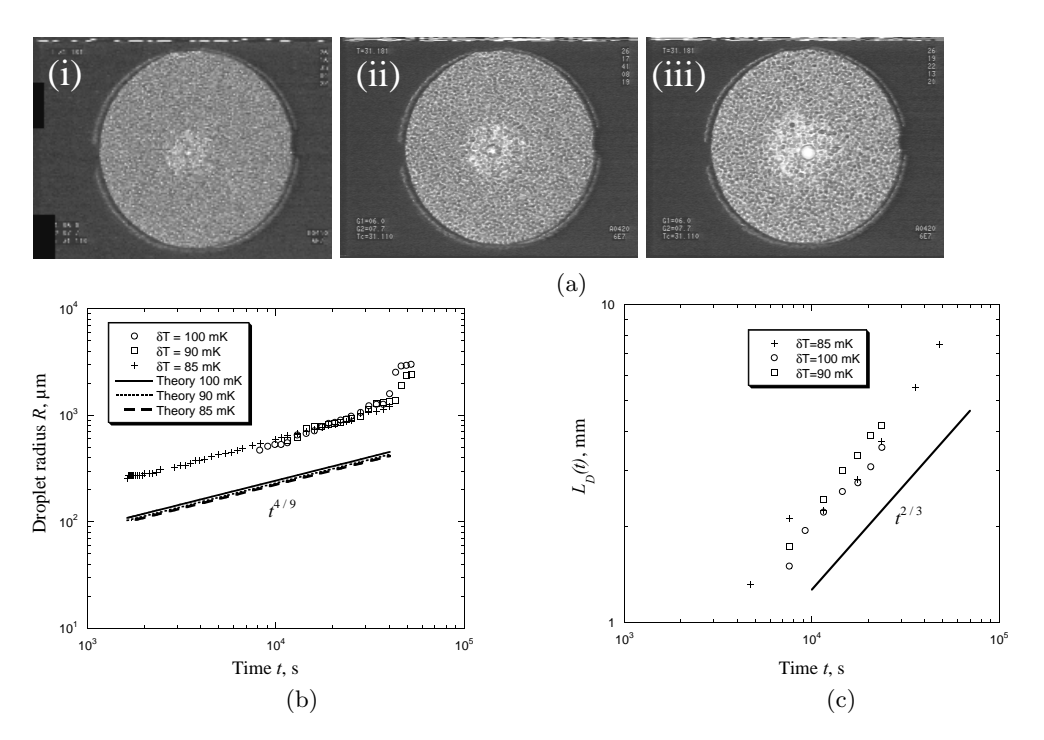


Fig. 3 – Growth of a single CO<sub>2</sub> gas bubble trapped by the beam for the quench depth  $\delta T=90$  mK. (a) Time evolution of the pattern: (i) t = 7207 s, (ii) t = 11580 s, and (iii) t = 17640 s. Note also the growth of the depletion zone centered around the growing bubble. (b) Experimental growth laws of the gas bubble trapped by the laser beam and (c) of the depletion zone for  $\delta T=85,\,90,\,$  and 100 mK. The growth curves calculated using (17) are also plotted in (b). The theoretically predicted slope 2/3 is shown in (c) for comparison.

center, while small bubbles grow everywhere in the sample. Growth continues when the central bubble becomes larger than the beam illuminated area. The growth of the central bubble clearly generates in its vicinity a strong density depletion of small bubbles. In addition, this central bubble grows faster than the small bubbles. From the three experiments shown in Fig. 3b, we deduce that the evolution of the radius R of the single beam-trapped bubble is given by the power law  $R(\tau) \sim t^x$ , where  $x = 0.47 \pm 0.01$  for  $\delta T = 85$  mK,  $x = 0.56 \pm 0.11$  for  $\delta T = 90$  mK, and  $x = 0.67 \pm 0.04$  for  $\delta T = 100$  mK. When calculating these exponents, we do not consider the very late times data when the bubble diameter reaches the cell thickness and

4 EUROPHYSICS LETTERS

the bubble begins a lateral motion out of the beam center. This motion is due to a driving force that appears when the bubble is squeezed between the cell windows that are not strictly parallel. In microgravity, even a very small angle is sufficient to move a squeezed bubble, see the discussion in [6]. There is a crossover to a much faster growth when the opposite windows of the cell become joined by this gas "bridge", see Fig. 3b. We will discuss this point later on.

The  $Q_m(\tau)$  curve which corresponds to the central bubble growth (with 2R used for  $L_m$ ) lies in between the two master curves in Fig.2. The average value for the exponent  $x \sim -0.5$  does not coincide with the exponent observed [2] in a phase separating binary mixture located in a thermal gradient induced by a Peltier element ( $Q_m(\tau) \sim \tau^{-2}$  during 15 s). The comparison between both experiments is difficult as the heat flow configuration is different. We however stress that our experiment lasts almost two decades in the scaled time, which makes the determination of a power law exponent quite reliable.

For the same three experiments, we have also analyzed the growth of the diameter  $L_D$  of the depletion zone (Fig. 3c). Results are, respectively,  $L_D(t) \sim t^{0.72\pm0.18}$ ,  $L_D(t) \sim t^{0.76\pm0.06}$ , and  $L_D(t) \sim t^{0.68\pm0.10}$ .

Theoretical model. - The observed beam trapping as well as the enhancement of the coarsening process can be explained by a Marangoni effect caused by a temperature variation at the bubble interface. A question arises whether such a variation can exist in a true singlecomponent system. There is strong evidence [6] that when the liquid-gas interface is initially at saturation conditions, the interface is isothermal unless a contamination is present in the fluid [7]. However, in the present work, the system is already out of equilibrium at the initial moment of time (i.e. during the quench). A strong density variation forms at the beginning of the evolution. We consider the "late" stages during which the bubble interfaces are already well formed and the density variation in the bulk of the phases is smaller, but still exists. Since the pressure of the system is equilibrated quickly after the quench due to the piston effect [8], the system evolves along the metastable branches of the isobar shown in Fig. during most of the evolution time. The liquid phase is overheated and the gas is overcooled. Therefore, the interface temperature is not necessarily equal to the saturation temperature (i.e.  $T_f$ ) that corresponds to the system pressure. It can thus vary along the bubble interface. One can estimate the upper limit for this variation as a difference  $\Delta T$  between the maximum overheating and minimum undercooling temperatures, see Fig. . Despite the presence of this (small) spatial density variation, the associated Lifshitz-Slyozov mechanism of bubble growth is not relevant. The kinetics turns out to be dominated by the droplet diffusion and coalescence (Binder-Stauffer mechanism), see [3].

For a small temperature inhomogeneity, the velocity  $\vec{v}$  of thermocapillary migration of a bubble suspended in a fluid phase is proportional [9] to the externally imposed temperature gradient  $\vec{\nabla}T$ :

$$\vec{v} = -\frac{2}{2\eta_o + 3\eta_i} \frac{\mathrm{d}\sigma}{\mathrm{d}T} \frac{a}{2 + \lambda_i/\lambda_o} \vec{\nabla}T, \tag{1}$$

where  $\eta_o$  and  $\lambda_o$  (respectively  $\eta_i$  and  $\lambda_i$ ) are the viscosity and the thermal conductivity outside (respectively inside) the bubble of radius a. Here the surface tension  $\sigma$  decreases with temperature so that  $d\sigma/dT < 0$ . According to (1), the bubble should migrate along the temperature gradient. Since in our case heating is localized inside the laser beam, the bubbles should migrate towards its center, coalescing between each other. The formation of the centered single bubble provides a qualitative demonstration of the above theory.

In order to develop a quantitative approach, we need to determine the gradient  $\nabla T$  induced

by the beam with the Gaussian radial intensity distribution

$$I(r) = \frac{2P}{\pi\omega^2} e^{-2r^2/\omega^2} \tag{2}$$

at the entrance of the cell. Here P is the beam power and r is the coordinate measured radially from the beam center.

The beam path in the cell consists of (i) a thin absorbing layer on the sapphire-fluid boundary that absorbs the power  $\gamma P$ , (ii) a non-absorbing layer of  $\mathrm{CO}_2$ , and (iii) an absorbing layer equivalent to (ii). There is only one trapped bubble on the entrance window because, during the quench, the bubbles that are forming in the bulk fluid scatter so much light that the laser beam is strongly attenuated before reaching the second window.

Due to the small ratio thickness/radius of the experimental cell, we will assume that the temperature distribution is of cylindrical symmetry with the axis along the beam as in [10]. In other words, we make the simplifying assumption that the power is dissipated homogeneously along the part of the beam that crosses the fluid, so that the heat power j generated per unit volume of the fluid is  $j(r) = 2\gamma I(r)/L$ .

For a long observation time we can also reasonably assume that the Piston effect is negligible and the temperature distribution is given by the stationary heat conduction equation

$$\lambda_o \nabla^2 T + j = 0. (3)$$

Note that this bubble trapping can be influenced by a dipolar ("optical trapping") effect [11] that appears because the refractive index of a gas bubble is smaller than that of the liquid phase. Then the dipolar forces act against the thermocapillary trapping by expulsing bubbles from the illuminated region. This effect is, however, negligibly small for the beam parameters used here. In addition, it is proportional to  $|\mathrm{d}I/\mathrm{d}r|$  and thus follows the exponential decline of the beam intensity (2) at large r.

The solution of (3) results in the radial temperature gradient

$$|\vec{\nabla}T| = \frac{\partial T}{\partial r} = -\frac{\gamma P}{\pi r L \lambda_o} \left( 1 - e^{-2r^2/\omega^2} \right). \tag{4}$$

The velocity  $\vec{v}$  as given by (1) behaves as

$$v = a\beta/r \tag{5}$$

outside the illuminated area and is directed towards the center of the beam (i.e. opposite to the r axis). The constant  $\beta$  is defined by

$$\beta = \frac{1}{2\eta_o + 3\eta_i} \left| \frac{\mathrm{d}\sigma}{\mathrm{d}T} \right| \frac{1}{2\lambda_o + \lambda_i} \frac{2\gamma P}{\pi L}.$$
 (6)

For the temperature  $T_f = T_c - 139.6$  mK that corresponds to the  $\delta T = 90$  mK quench,  $\beta = 0.173 \,\mu\text{m/s}$ .

One can now obtain the growth law for the central bubble based on the expression (5). Let us denote by c = c(r) the number of (small) gas bubbles in the unit volume. The total flux  $\vec{f} = \vec{f}(r)$  of the bubbles (i.e. the average number of the bubbles that cross the unit area per unit time)

$$\vec{f}(r) = -D\vec{\nabla}c + c\vec{v},\tag{7}$$

has two contributions. The first term corresponds to the diffusion of the bubbles with the diffusion constant D, while the second is responsible for the drift with the average velocity  $\vec{v}$  in

6 EUROPHYSICS LETTERS

the external force field. In our case, the latter corresponds to the thermocapillary migration of the bubbles. Under the assumption of a nearly stationary distribution for c(r),  $\vec{f}(r)$  satisfies the equation

$$\operatorname{div}\vec{f} = 0. \tag{8}$$

Since the thickness L of the cell is much smaller than its diameter, the motion of the bubbles towards the beam center is almost 2D. Indeed, Fig. 3c shows that the scale  $L_D$  of the c(r) variation can be 3 times larger than L. Therefore, Eqs. (7-8) should be solved in 2D, i.e. for a function c(r) with a cylindrical symmetry. However, the central bubble is spherical because of the surface tension and cannot be assumed cylindrical. To solve this contradiction, we introduce a cylindrical bubble of radius  $R_{2D}$  which has the same volume  $V_R$  as the actual central bubble with the radius R,

$$V_R = \frac{4\pi}{3}R^3 = \pi R_{2D}^2 L. \tag{9}$$

In the cylindrical coordinates, (8) reduces to the 2nd order ordinary differential equation

$$\frac{\mathrm{d}}{\mathrm{d}r} \left[ r \left( -D \frac{\mathrm{d}c}{\mathrm{d}r} - \frac{ca\beta}{r} \right) \right] = 0. \tag{10}$$

Assuming that a is independent of r (i.e. that the rate of collisions is not influenced by the weak gradient of bubble concentration c), Eq. (10) can be solved with two boundary conditions  $c(R_{2D}) = 0$  (that corresponds to the disappearance of the small bubbles when they touch the central bubble) and  $c(\infty) = c_{\infty}$ , the constant bubble concentration at infinity. The solution of (10) reads

$$c(r) = c_{\infty} [1 - (r/R_{2D})^{-a\beta/D}] \tag{11}$$

and shows a depletion zone, that can be defined as the zone of  $0 < r \le L_D/2$  where  $c(r) \le 0.9 c_{\infty}$ . According to (11), this condition results in

$$L_D \sim R_{2D} \sim t^{2/3},$$
 (12)

which fits the experimental data, see Fig. 3c.

The central hemispherical bubble grows at the expense of the small bubbles that are absorbed by coalescence, so that

$$dV_R/dt = 2\pi R_{2D} Lf(R_{2D})V_a, \tag{13}$$

where  $f(R_{2D}) = c_{\infty} \beta a / R_{2D}$  and  $V_a$  is the volume of a small bubble. The product  $c_{\infty} V_a$  is the constant vapor volume fraction  $\phi = (\rho_L - \rho)/(\rho_L - \rho_V)$ ,  $\rho_L$  and  $\rho_V$  being defined in Fig. . Eq. (13) then reduces to

$$R_{2D} \, \mathrm{d}R_{2D} / \mathrm{d}t = \beta \phi a. \tag{14}$$

The growth law for the small bubbles is

$$a = a_0 t^{1/3} (15)$$

with  $a_0$  that follows from eq.  $Q_m(\tau) = 0.95\tau^{-1/3}$  and the relationship [12]  $\phi = 0.69 (L_m/2a)^{-3}$ ,

$$a_0 = 1.91 \, \phi \left(\frac{k_B T_c}{\eta_o}\right)^{1/3} \,.$$
 (16)

For the  $\delta T = 90$  mK quench,  $a_0 = 1.38 \cdot 10^{-6}$  ms<sup>-1/3</sup>. Eqs. (9,14,15) result in the growth laws

$$R_{2D} = \sqrt{3\beta\phi a_0/2} t^{2/3}, \quad R = (9L\beta\phi a_0/8)^{1/3} t^{4/9}.$$
 (17)

The R(t) curve can now be plotted in Fig. 3b. The theoretical curve fits the experimental data within a constant factor  $\approx 2$ . In addition, its experimentally observed week dependence on  $\delta T$  is reproduced well by the model. Such a good agreement obtained in spite of several assumptions confirms the Marangoni origin of the fast growth of the cental bubble.

The crossover to the faster kinetics visible in Fig. 3b can now be understood. It is observed when the central bubble joins the opposite cell windows. One can assume that this crossover has a geometrical origin. Indeed, if the bubble became exactly cylindrical, its growth exponent would be that of  $R_{2D}$ , i.e. the growth would accelerate. However, the actual growth law after crossover is difficult to obtain since the actual shape of this bubble squeezed between the windows is complicated, see [6].

Concluding remark. – This work shows that even a weak temperature gradient can strongly modify the kinetics of phase transitions and affect material processing. In addition, this work presents a clear evidence of the temperature gradient along the gas-liquid interface in a truly one-component fluid systems. While the Marangoni convection caused by such gradients is commonly observed in presence of a second fluid, clear evidence of such an effect in a pure fluid is unknown to us.

## REFERENCES

- [1] N. O. Young, J. S. Goldstein, and M. J. Block, J. Fluid Mech. 6, 350 (1959).
- B. Braun, C. Ikier, H. Klein, and D. Woermann, J. Colloid Interface Sci. 159, 515 (1993); B. Braun, C. Ikier, H. Klein, and D. Woermann, Chem. Phys. Lett. 233, 565 (1995); C. Ikier, H. Klein, and D. Woermann, J. Colloid Interface Sci. 184, 693 (1996).
- [3] F. Perrot, P. Guenoun, T. Baumberger, D. Beysens, Y. Garrabos, and B. Le Neindre, Phys. Rev. Lett. 73, 688 (1994).
- [4] J.-M Laherrère and P. Koutsikides, Acta Astronautica 29, 861 (1993).
- [5] Highlights of the Zeno Results from the USMP-2 Mission, Zeno Home Page at http://roissy.umd.edu/report/report.html.
- [6] Y. Garrabos, C. Lecoutre-Chabot, J. Hegseth, V.S. Nikolayev, D. Beysens, Phys. Rev. E 64, 051602 (2001).
- [7] R. Marek, J. Straub, Int. J. Heat Mass Transfer 44, 619 (2001).
- [8] Y. Garrabos, M. Bonetti, D. Beysens, F. Perrot, T. Fröhlich, Phys. Rev. E 57, 5665 (1998).
- [9] K. D. Barton and R. S. Subramanian, J. Colloid Interface Sci. 133, 211 (1989).
- [10] A. Marcano O. and L. Aranguren, Appl. Phys. B 56, 343 (1993).
- [11] J.-P. Delville, C. Lalaude, S. Buil, and A. Ducasse, Phys. Rev. E 59, 5804 (1999).
- [12] V. S. Nikolayev, D. Beysens and P. Guenoun, Phys. Rev. Lett. **76**, 3144 (1996).